Manchester Metropolitan University

e-space

Manchester Metropolitan University's Research Repository

Please cite the Published Version

Milosavljević, M, Shao, G, Loureo, MA, Gwilliam, RM, Homewood, KP, Edwards, SP, Valizadeh, R and Colligon, JS (2005) Transition from amorphous to crystalline beta phase in co-sputtered Fe Si2 films as a function of temperature. Journal of Applied Physics, 98 (12). p. 123506. ISSN 0021-8979

DOI: https://doi.org/10.1063/1.2148629

Publisher: AIP Publishing

Version: Published Version

Downloaded from: https://e-space.mmu.ac.uk/94402/

Additional Information: This article may be downloaded for personal use only. Any other use requires prior permission of the author and AIP Publishing. This article appeared in M. Milosavljević, G. Shao, M. A. Lourenço, R. M. Gwilliam, K. P. Homewood, S. P. Edwards, R. Valizadeh, and J. S. Colligon, "Transition from amorphous to crystalline beta phase in co-sputtered FeSi2 films as a function of temperature", Journal of Applied Physics 98, 123506 (2005) and may be found at https://aip.scitation.org/doi/10.1063/1.2148629

Enquiries:

If you have questions about this document, contact openresearch@mmu.ac.uk. Please include the URL of the record in e-space. If you believe that your, or a third party's rights have been compromised through this document please see our Take Down policy (available from https://www.mmu.ac.uk/library/using-the-library/policies-and-guidelines)

JOURNAL OF APPLIED PHYSICS **98**, 123506 (2005)

Transition from amorphous to crystalline beta phase in co-sputtered $FeSi_2$ films as a function of temperature

M. Milosavljević
Advanced Technology Institute, School of Electronics and Physical Sciences, University of Surrey, Guildford, Surrey GU2 7XH, United Kingdom, and VINČA Institute of Nuclear Sciences, Belgrade, Serbia and Montenegro

G. Shao[a]
BCAST—Brunel Centre for Advanced Solidification Technology, Brunel University, Uxbridge UB8 3PH, United Kingdom

M. A. Lourenço, R. M. Gwilliam, and K. P. Homewood
Advanced Technology Institute, School of Electronics and Physical Sciences, University of Surrey, Guildford, Surrey GU2 7XH, United Kingdom

S. P. Edwards
School of Engineering, University of Surrey, Guildford, Surrey GU2 7XH, United Kingdom

R. Valizadeh and J. S. Colligon
Department of Chemistry and Materials, Manchester Metropolitan University, Manchester, M1 5GD, United Kingdom

(Received 16 June 2005; accepted 10 November 2005; published online 21 December 2005)

A study of the stability of amorphous $FeSi_2$ films and their transition to a crystalline phase as a function of deposition or annealing temperature is presented. Stoichiometric $FeSi_2$ films, 300–400 nm thick, were deposited on (100) Si substrates by co-sputtering of Fe and Si. It was found that the films grow in an amorphous form for the substrate temperature ranging from room temperature to 200 °C, while from 300–700 °C, they grow in form of a crystalline β-$FeSi_2$ phase. In a postdeposition 30 min heat treatments, the layers retain the amorphous structure up to 400 °C, transforming to the crystalline β phase at 500–700 °C. The results are discussed in the frame of the existing models, and compared to those found in the literature. It is shown that in as-deposited films, the growth is controlled by surface diffusion, the crystalline layers growing in a columnar structure strongly correlated to the Si substrate. Postdeposition treatments induce a random crystallization controlled by bulk diffusion, the resulting structure not being influenced by the substrate. The results of this work contribute to a better understanding of the processes involved in a transition of amorphous $FeSi_2$ films to a crystalline phase, and provide a basis to determine the processing parameters in potential applications of this promising semiconducting material. © *2005 American Institute of Physics*. [DOI: 10.1063/1.2148629]

I. INTRODUCTION

Crystalline β-$FeSi_2$ films have attracted significant attention as a direct band gap semiconducting material, of E_g $=0.85-0.87$ eV.[1,2] Such properties allowed successful fabrication of a silicon-based light-emitting device,[3] consisting of β-$FeSi_2$ precipitates in a Si matrix, thus opening potential routes for optical interconnects in silicon integrated circuit technology. Apart from this β-$FeSi_2$ has a high photoabsorption coefficient, about 50 times higher than crystalline Si, making it suitable for fabrication of high efficiency solar cells.[4] Recently, we have reported[5,6] the existence of another semiconductor: the amorphous form of $FeSi_2$. The material was initially synthesized by ion beam mixing of Fe films on Si substrates and later confirmed by co-sputter deposition of iron and silicon.[7] Amorphous $FeSi_2$ is also a direct gap semiconductor with a band gap of 0.88–0.90 eV, close to that of the crystalline β phase, and with a similar photoabsorption efficiency. More recently,[8] it was reported that very fine (3–5 nm) nanocrystalline β-$FeSi_2$ films also exhibit a direct band gap behavior. As their structure is somewhere at the boundary between a fully grown crystalline and the amorphous $FeSi_2$ phase, the measured E_g=0.85–0.95 eV confirms similar band gap values for these two phases. Evidently, amorphous layers can be deposited on any surface, and hence there is a promising potential for applications of iron disilicide in large area electronics and for fabrication of solar cells.

Various growth methods and the properties of crystalline β films were studied extensively, but there is little evidence on the studies of amorphous iron disilicide. There are earlier reports[9,10] on the studies of electrical conductivity of these films, but their optoelectronic properties were not considered. There is also a report[11] on photoelectron spectroscopy of these films, and more recently,[12] their vibrational density of states were studied and compared to those of crystalline β layers. Previously we have reported[7] on the possibility to

[a]Author to whom correspondence should be addressed; electronic mail: mestggs@brunel.ac.uk

 © 2005 American Institute of Physics

Downloaded 11 May 2009 to 131.227.178.132. Redistribution subject to AIP license or copyright; see http://jap.aip.org/jap/copyright.jsp

modify optical absorption of amorphous $FeSi_2$ films by applying a higher deposition temperature or by ion irradiation. However, further investigations of the basic properties of this material are needed to verify its viability for potential applications.

In this article, we concentrate on the growth conditions and stability of amorphous $FeSi_2$ films, and on their transformation to a crystalline phase with respect to deposition or annealing temperature. Stoichiometric $FeSi_2$ films were grown on (100) Si substrates by co-sputtering of Fe and Si. The obtained results suggest that the growth of as-deposited layers is controlled by surface diffusion, the layers growing in an amorphous form for the substrate temperature ranging from ambient (RT) to 200 °C. On the other hand, crystallization of initially amorphous layers is controlled by bulk diffusion, and they retain an amorphous structure up to 400 °C. The results are discussed in the framework of the existing models and compared to those found in the literature. They show a possibility to control the layer structure, and suggest a temperature interval that can be used for processing and modification of amorphous $FeSi_2$ films.

II. EXPERIMENTAL SETUP

Iron disilicide films were prepared in a vacuum chamber designed for ion-beam-assisted deposition (IBAD), having a base pressure in the 10^{-7} mbar range. The system is equipped with two low-energy Ar ion guns, one for sputtering the target material and the other for irradiating the substrate during deposition. The substrate holder has a thermocouple-controlled heating stage of up to 900 °C. We have used a target composed of Fe and Si plates, arranged to give the $FeSi_2$ stoichiometry of the deposit. For these experiments we only used one ion gun for sputtering, while the other gun was used just for cleaning the substrates before deposition. The substrates used were (100) Si wafers, prepared by a standard dip in an HF solution and in deionized water before mounting in the chamber. The $FeSi_2$ layers were deposited at a rate of 0.07 nm/s, to a thickness of 300–400 nm. The substrate temperature was varied from RT to 700 °C, in steps of 100 °C. A more detailed description of the IBAD system is given elsewhere.[13]

Postdeposition heat treatment of the samples deposited at RT was performed by rapid thermal annealing, in a nitrogen ambient, for 30 min at temperatures ranging from 300 to 700 °C, in steps of 100 °C. Stoichiometry of the layers and uniformity of Fe and Si depth profiles were analyzed by Rutherford backscattering spectroscopy (RBS), using a 1.5 MeV He^+ ion beam. Structural analysis was done by transmission electron microscopy (TEM), using Philips EM 400 T and CM 200 microscopes, operated at 120 and 200 keV, respectively. We have performed cross-sectional TEM analysis (XTEM), and selected area diffraction and microdiffraction (MD) analysis to identify the phases. We also carried out energy dispersive x-ray spectroscopy (EDX) with a nanobeam probe to verify the layer composition and uniformity.

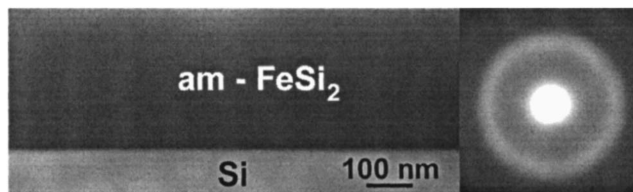

FIG. 1. Bright-field XTEM image of amorphous $FeSi_2$ film annealed at 400 °C, taken near [110] Si. Inset is a MD pattern taken from the film.

III. RESULTS

The results of XTEM analysis revealed that the $FeSi_2$ films deposited at RT, 100 °C, and 200 °C have an amorphous structure. The same is true for samples deposited at RT and subsequently annealed at 300 and 400 °C. A typical analysis that demonstrates this structure is illustrated in Fig. 1. It shows a bright-field XTEM image and the corresponding MD pattern of an amorphous $FeSi_2$ layer annealed at 400 °C. The image was taken near the [110] Si zone axis. It shows a featureless structure of the layer, with a smooth surface and a sharp interface towards the Si substrate. No indication of the presence of nanocrystals could be seen for different sample tilts in diffraction-contrast imaging. The MD pattern taken from the $FeSi_2$ layer shows a typical hallow ring of an amorphous structure. Analysis of other amorphous samples gave similar results.

For substrate temperatures ranging from 300 to 700 °C, the as-deposited films grow in the form of a polycrystalline β-$FeSi_2$ phase. Figure 2 presents a bright-field XTEM image of a layer deposited at 300 °C and a dark-field image of a layer deposited at 500 °C. It is seen that the layers grow in a columnar structure, with individual crystal grains stretching from the Si substrate to the surface. Lateral dimensions of the grains increase from 30 to 50 nm for the deposition temperature of 300 °C up to above 100 nm for the higher deposition temperature. A detailed electron diffraction analysis has identified these grains as β-$FeSi_2$ crystals. The MD patterns presented in the figure were taken from a single grain in each case. The [011] β-$FeSi_2$ orientation in (a) was found close to [110] Si zone axis, where we also found $[1\bar{1}2]$ oriented β grains. For the higher deposition temperature, the β

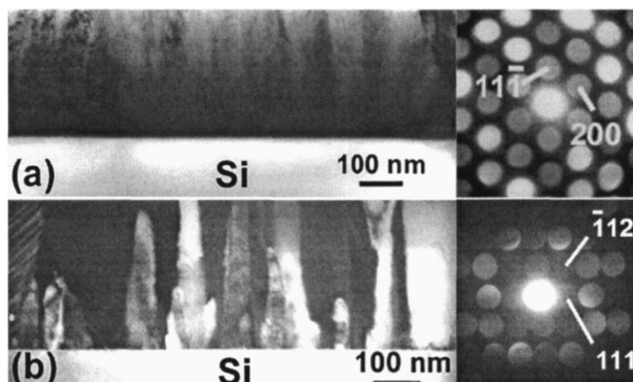

FIG. 2. Bright-field XTEM image (a) of an as-deposited film at 300 °C, and dark-field XTEM image (b) of an as-deposited film at 500 °C. The corresponding MD patterns were taken from a single β–$FeSi_2$ grain in each case.

Downloaded 11 May 2009 to 131.227.178.132. Redistribution subject to AIP license or copyright; see http://jap.aip.org/jap/copyright.jsp

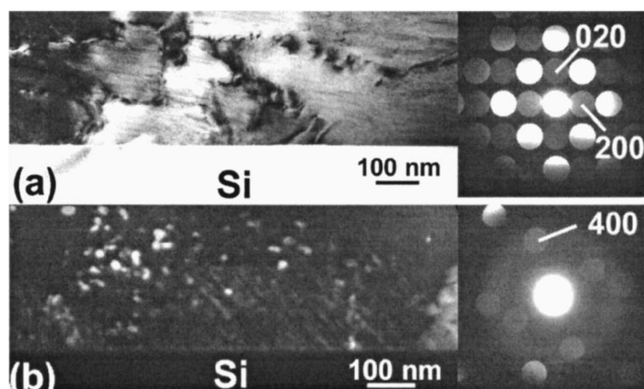

FIG. 3. XTEM analysis of initially amorphous films: bright-field image (a) of a sample annealed at 500 °C, and dark-field image (b) of a sample annealed at 600 °C. MD patterns identify a β-$FeSi_2$ grain (a) and a diffraction ring originating from β-$FeSi_2$ nanocrystals (b).

grains are oriented slightly off the main Si zone axis, the [$1\bar{3}2$] β-$FeSi_2$ shown in (b) being ~3° off [110] Si.

In Fig. 3 we present XTEM analysis of initially amorphous $FeSi_2$ layers after their annealing at 500 and 600 °C. The identified phase is β-$FeSi_2$, but the layer structure is markedly different compared to the layers deposited at these temperatures. As seen from the bright-field XTEM image taken from the sample annealed at 500 °C, the layers crystallize in form of relatively large grains of up to a few hundred nm with a random orientation, practically not influenced by the Si substrate. The enclosed MD pattern shows a [001] orientation of a β-$FeSi_2$ grain, which was found far away from any low-index Si planes. These relatively large grains have irregularly shaped grain boundaries, some of them containing β-$FeSi_2$ nanocrystals. Some of the large grains also contain β-$FeSi_2$ nanocrystals, as seen in the dark-field image taken from a sample annealed at 600 °C. Nanocrystals appear as bright features in the image and give a sharp diffraction ring in the MD pattern taken from this area. The pattern was taken off a main crystal zone axis, as the contrast of the ring is rather weak. The position of the ring coincides with the strong (400) reflection from a larger β-$FeSi_2$ grain.

The effect of increasing the substrate temperature to 700 °C is illustrated in Fig. 4, showing bright-field XTEM images of an as-deposited and an annealed sample, both taken near [110] Si. The as-deposited layer grows in the form of much larger β-$FeSi_2$ grains compared to the lower deposition temperatures, resulting in a pronounced surface topography. The growth is still strongly influenced by the substrate, although the grains are more relaxed and oriented 4°–5° off [110] Si. The annealed layer crystallizes also in form of large β-$FeSi_2$ grains, but again their crystallographic orientation is not influenced by the substrate. The surface of the layer remains smooth, although larger grains still contain nanocrystals of the same phase. A partial lift off from the substrate can be seen at the grain boundary, suggesting that internal stress builds up in the layer during crystallization.

RBS analysis has shown uniform Fe and Si depth profiles in all as-deposited and annealed samples, with a concentration ratio within 1–2 at. % of $FeSi_2$ stoichiometry. An example is given in Fig. 5, showing a random near-normal

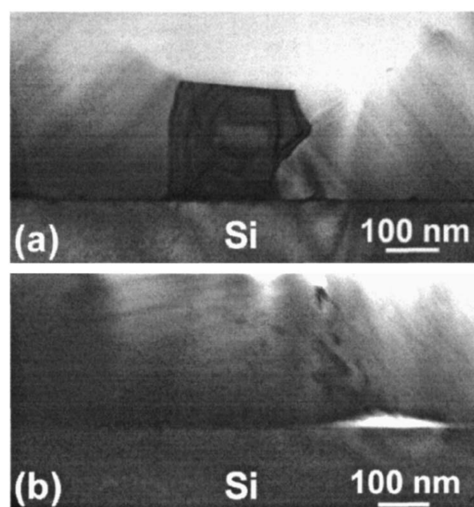

FIG. 4. Bright-field XTEM images from: (a) as-deposited film at 700 °C, and (b) initially amorphous film annealed at 700 °C.

incidence RBS spectrum taken from a sample deposited at RT. Simulation of the spectrum gave the exact $FeSi_2$ stoichiometry, and taking the bulk density of β-$FeSi_2$ (7.95×10^{22} at./cm^3), the calculated layer thickness of 310 nm matched the value measured by XTEM. Similar spectra were obtained from crystalline samples deposited at higher temperatures, and from the samples that crystallized during annealing. As in RBS, the analyzing beam gives, on average, information from an area of ~1 mm diameter, we also did EDX spectroscopy of cross-sectional samples in TEM, using a nanobeam probe. In this case, the analyzing beam was smaller than individual grains in the crystalline layers. Stoichiometry of the layers, analyzed at various spots on the samples, was consistent with RBS results. Figure 6 shows the Fe elemental map (using a scanning e-beam) of a sample as-deposited at 300 °C, and the elemental composition taken at a mid-depth of the $FeSi_2$ layer. Elemental maps were similar for all amorphous and crystalline samples, suggesting uniform distribution of Fe and Si within the layers on a nanometer scale. Elemental analysis shows Fe and Si peaks, and a low Cu peak originating from the sample holder in

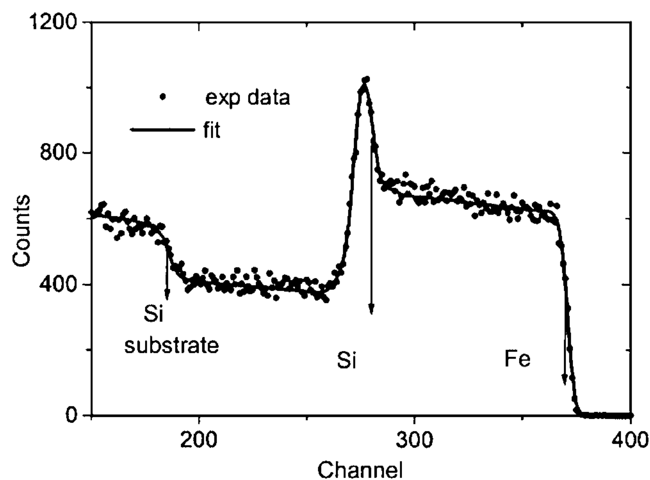

FIG. 5. RBS analysis of $FeSi_2$ film deposited at RT, showing a random experimental spectrum near [100] Si and the simulation fit.

Downloaded 11 May 2009 to 131.227.178.132. Redistribution subject to AIP license or copyright; see http://jap.aip.org/jap/copyright.jsp

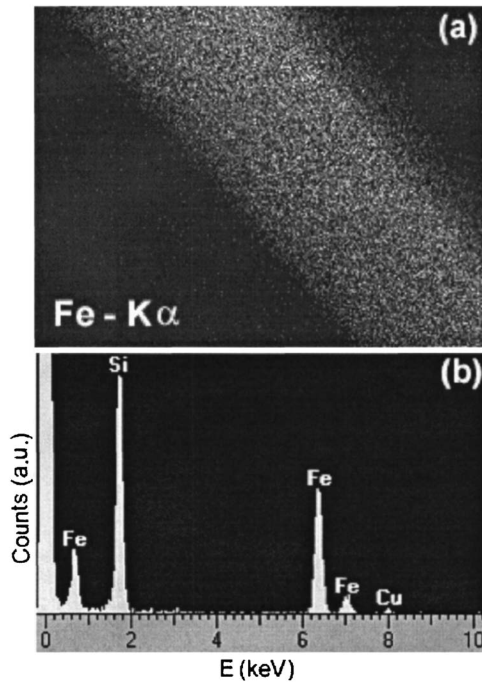

FIG. 6. EDX map of Fe in an as-deposited film at 300 °C (a), and elemental analysis from a midposition of the film (b).

TEM. The presence of other contaminants is below the detection limit of the system. In the particular case presented in Fig. 6(b), the deduced Fe:Si composition was ~32:68.

IV. DISCUSSION

The results of TEM analysis suggest that the growth and crystallization in as-deposited $FeSi_2$ layers is controlled by surface diffusion. For the substrate temperature from RT to 200 °C, the adsorbed atomic species have insufficient mobility for crystallization. At 300 °C and higher temperatures, their mobility enables them to diffuse at the substrate surface and form a crystalline structure. As the atomic ratio of deposited species satisfies the $FeSi_2$ stoichiometry, the crystalline phase that forms is the low-temperature β-$FeSi_2$. This phase is known to be stoichiometric, with an allowed 1–2 at. % of Fe or Si vacancies, while the high-temperature α and the metastable γ phases generally have a much higher concentration of vacancies. There are close epitaxial relationships between β-$FeSi_2$ and crystalline Si, as discussed, for example, in Ref. 14. Hence, the as-deposited layers grow in the form of smaller or larger epitaxial grains, depending on the substrate temperature. Higher temperatures yield larger and more relaxed grains, allowing for their slight rotation due to a lattice mismatch with Si. Columnar structure suggests a layer by layer growth, when initially nucleated grains act as seeds for homoepitaxy. In the films deposited at 700 °C the adsorbed atoms have a sufficient mobility to follow the structure of large underlaying grains, resulting in a developed surface morphology.

An effective surface diffusion distance $\bar{x}$ of adsorbed atomic species in physical vapor deposition can be deduced from[15,16]

TABLE I. Effective surface diffusion distance $\bar{x}$ in $FeSi_2$ films as a function of deposition temperature T, the surface diffusion coefficient D_s, and the deposition rate R. Different values of $\bar{x}$ at the same temperature are due to different deposition rates.

T (K)	D_s (m^2/s)	R (nm/s)	$\bar{x}$ (nm)	Comment
293	1.15×10^{-29}	0.07	7.04×10^{-6}	Crystallization suppressed
373	5.86×10^{-25}	0.07	0.0016	
473	2.58×10^{-21}	0.07	0.1051	
573	6.06×10^{-19}	0.07	1.6118	Crystallization possible (This work)
773	4.84×10^{-16}	0.07	45.548	
973	2.48×10^{-14}	0.07	325.88	
473	2.58×10^{-21}	0.3	0.0508	Crystallization suppressed
597	1.71×10^{-18}	0.3	1.3085	Crystallization possible (Ref. 10)
293	1.15×10^{-29}	0.03	1.04×10^{-5}	Crystallization suppressed
773	4.84×10^{-16}	0.03	69.570	Crystallization possible (Ref. 12)
573	6.06×10^{-19}	0.02	3.0149	Crystallization possible (Ref. 18)

$$\bar{x} = \sqrt{D_s \frac{\alpha}{R}}, \tag{1}$$

where D_s is the surface diffusion coefficient, α is the interatomic spacing, and R is the deposition rate.

Surface diffusivity of metallic systems can be approximated as[17]

$$D_s \approx 10^{-7} \exp\left(-10\frac{T_m}{T}\right), \tag{2}$$

where T_m is the solid→liquid transformation temperature (1480 K for β-$FeSi_2$) and T the substrate temperature. Taking an average value of α=0.3 nm and the deposition rate of 0.07 nm/s, the calculated values of $\bar{x}$ are given in Table I. When $\bar{x}$ is greater than the unit cell of a competing crystalline phase (~0.8 nm for $FeSi_2$), crystallization during deposition is possible.

Although rather simplified, and not taking into account different diffusivity for Fe and Si, the calculated data are in very good agreement with our experimental results and those found in the literature.[10,12,18] However, when a highly energetic pulsed laser deposition technique is used,[8,19] the films grow in the form of a nanocrystalline β-$FeSi_2$ phase already at RT. In the studies of this technique for deposition of β-$FeSi_2$ it was suggested[19] that diffusivity of Si atoms is dominant for substrate temperatures ⩾400 °C, and diffusivity of Fe atoms is enhanced for substrate temperatures ⩾700 °C. Although this may be more related to bulk diffusion in already deposited material in short pulses, perhaps it

Downloaded 11 May 2009 to 131.227.178.132. Redistribution subject to AIP license or copyright; see http://jap.aip.org/jap/copyright.jsp

TABLE II. The mean bulk diffusion length $\bar{l}$ in $FeSi_2$ as a function of annealing temperature T, the bulk diffusion coefficient D_b and the annealing time t.

T (K)	D_b (m^2/s)	t (min)	$\bar{l}$ (nm)	Comment
573	1.84×10^{-27}	30	0.0044	Crystallization
673	3.96×10^{-24}	30	0.2067	suppressed
773	1.17×10^{-21}	30	3.5573	Crystallization
873	9.41×10^{-20}	30	31.885	possible
973	3.07×10^{-18}	30	182.083	(This work)
673	3.96×10^{-24}	60	0.2923	Crystallization observed (Ref. 10)

can be compared to our results. In our case crystallization at 300 °C may be due mainly to dominant mobility of Si atoms, while the growth of larger and more relaxed grains at 500–700 °C probably results from an overall mobility of both Si and Fe.

In case of the films that were deposited in an amorphous form, crystallization is controlled by bulk diffusion. Here, the diffusion coefficient can be approximated by[17,20]

$$D_b \approx 5 \times 10^{-5} \exp\left(-20\frac{T_m}{T}\right). \qquad (3)$$

An estimate of the mean diffusion length $\bar{l}$ can be obtained from the well known form:

$$\tilde{l} = \sqrt{6D_b t}, \qquad (4)$$

where t is the annealing time. The calculated values of $\bar{l}$, given in Table II, again show a very good agreement with our experimental results. In earlier studies of amorphous $FeSi_2$ films deposited on glass and sapphire substrates, it was suggested that crystallization occurs at 400–450 °C, although for a longer period of annealing[10] or for the annealing duration not defined,[9] and a microanalysis of fully crystallized layers at these temperatures was not presented. Our analysis shows that $FeSi_2$ films retain an amorphous structure after annealing for 30 min at 400 °C, while at 500 °C they fully transform to crystalline β-$FeSi_2$ phase. Having the $FeSi_2$ stoichiometry, the atomic species do not need to diffuse long distances, and perhaps only an enhanced mobility of Si atoms is sufficient for a complete crystallization. The resulting structure is different from that of the as-deposited crystalline layers, or from the structures that are generally obtained in solid phase epitaxy or reactive deposition epitaxy, when silicon is supplied from the substrate. Crystallization from an amorphous $FeSi_2$ phase proceeds randomly and practically with no influence from the Si substrate. In this random process nanocrystals of the same phase nucleate independently and remain incorporated in larger grains or at grain boundaries. Their presence is reduced with increasing the annealing temperature, but also a tensile stress builds up in the layers due to a different thermal expansion coefficient from that of the Si substrate.

In our earlier report[6] we have presented thermodynamic calculations of the amorphous $FeSi_2$ phase equilibrium with Si, using a recently developed model.[21] An amorphous structure can be synthesized in form of a "frozen liquid," which can be relaxed into more stable structures when energy is added to activate the system. In the latter case a form of atomic ordering is established in the structure, when the number of dangling bonds is reduced. Recently, it was reported[22,23] that a medium range order can be introduced in amorphous silicon by thermal treatments or by ion irradiation. In our previous studies we have shown that optical absorption of amorphous $FeSi_2$ layers increases when they are deposited at a higher temperature, or after ion irradiation.[7] This behavior was assigned to establishing a higher degree of short to medium range order within the amorphous structure. In the present study we define a temperature interval that can be used for physical vapor deposition or for thermal processing of amorphous $FeSi_2$ layers. In both cases an added energy can induce a more ordered and relaxed amorphous structure, which can have an effect on electronic properties of the material. Optical absorption studies as a function of annealing temperature will be presented in a following publication.

V. CONCLUSIONS

We have studied the growth and stability of co-sputtered amorphous $FeSi_2$ films and their transformation to a crystalline phase as a function of the deposition or annealing temperature. The as-deposited films grow in an amorphous form for the substrate temperature ranging from RT to 200 °C. After a postdeposition thermal treatment for 30 min the amorphous structure remains stable up to 400 °C.

For the substrate temperature ranging from 300–700 °C, the as-deposited films grow in form of a crystalline β-$FeSi_2$ phase. The growth is controlled by surface diffusion, strongly influenced by the Si substrate, and resulting in a columnar structure of the films. In a postdeposition annealing of initially amorphous films crystallization is controlled by bulk diffusion. The layers transform fully to a crystalline β-$FeSi_2$ phase at 500–700 °C, in a random process not influenced by the Si substrate. The resulting structure consists of randomly oriented crystal grains, containing nanocrystals of the same phase.

The results of this work contribute to a better understanding of the basic processes involved in the growth and crystallization of co-deposited $FeSi_2$ films, and indicate a temperature interval when the amorphous phase is stable. They can be useful in modification of the amorphous structure towards achieving a higher degree of short to medium range order, and in various processing procedures in a potential application of this material.

[1] M. C. Bost and J. E. Mahan, J. Appl. Phys. **58**, 2696 (1985).
[2] Z. Yang, K. P. Homewood, M. S. Finney, M. A. Harry, and K. J. Reeson, J. Appl. Phys. **78**, 1958 (1995).
[3] D. Leong, M. Harry, K. J. Reeson, and K. P. Homewood, Nature (London) **387**, 686 (1997).
[4] Y. Makita, Y. Nakayama, Y. Fukuzawa, S. N. Wang, N. Otogawa, Y. Suzuki, Z. X. Liu, M. Osamura, T. Ootsuka, T. Mise, and H. Tanoue, Thin Solid Films **461**, 202 (2004).

Downloaded 11 May 2009 to 131.227.178.132. Redistribution subject to AIP license or copyright; see http://jap.aip.org/jap/copyright.jsp

[5]M. Milosavljević, G. Shao, N. Bibić, C. N. McKinty, C. Jeynes, and K. P. Homewood, Appl. Phys. Lett. **79**, 1438 (2001).
[6]M. Milosavljević, G. Shao, N. Bibić, C. N. McKinty, C. Jeynes, and K. P. Homewood, Nucl. Instrum. Methods Phys. Res. B **188**, 166 (2002).
[7]M. Milosavljević, G. Shao, R. M. Gwilliam, Y. Gao, M. A. Lourenco, R. Valizadeh, J. S. Colligon, and K. P. Homewood, Thin Solid Films **461**, 72 (2004).
[8]T. Yoshitake, M. Yatabe, M. Itakura, N. Kuwano, Y. Tomokiyo, and K. Nagayama, Appl. Phys. Lett. **83**, 3057 (2003).
[9]M. Komabayashi, K. Hijikata, and S. Ido, Jpn. J. Appl. Phys., Part 1 **30**, 563 (1991).
[10]M. Powalla and K. Herz, Appl. Surf. Sci. **65/66**, 482 (1993).
[11]R. Kilper, St. Teichert, Th. Franke, P. Häussler, H.-G. Boyen, A. Cossy-Favre, and P. Oelhafen, Appl. Surf. Sci. **91**, 93 (1995).
[12]M. Walterfang, W. Keune, E. Schuster, A. T. Zayak, P. Entel, W. Sturhahn, T. S. Toellner, E. E. Alp, P. T. Jochym, and K. Parlinski, Phys. Rev. B **71**, 035309 (2005).
[13]C. N. McKinty, A. K. Kewell, J. S. Sharpe, M. A. Lourenco, T. M. Butler, R. Valizadeh, J. S. Colligon, K. J. Reeson-Kirkby, and K. P. Homewood, Nucl. Instrum. Methods Phys. Res. B **161**, 922 (2000).
[14]G. Shao and K. P. Homewood, Intermetallics **8**, 1405 (2000).
[15]B. Cantor and R. W. Cahn, Acta Metall. **24**, 845 (1976).
[16]N. Saunders and A. P. Miodownik, J. Mater. Sci. **22**, 629 (1987).
[17]G. Shao and P. Tsakiropoulos, Philos. Mag. A **80**, 693 (2000).
[18]R. Kuroda, Z. Liu, Y. Fukuzawa, Y. Suzuki, M. Osamura, S. Wang, N. Otogawa, T. Ootsuka, T. Mise, Y. Hoshino, Y. Nakayama, H. Tanoue, and Y. Makita, Thin Solid Films **461**, 34 (2004).
[19]T. Yoshitake, T. Nagamoto, and K. Nagayama, Thin Solid Films **381**, 236 (2001).
[20]A. Cottrel, *An Introduction to Metallurgy*, 2nd ed. (Edward Arnold, London, 1975).
[21]G. Shao, J. Appl. Phys. **88**, 4443 (2000).
[22]P. M. Voyles, J. E. Gerbi, M. M. J. Treacy, J. M. Gibson, and J. R. Abelson, Phys. Rev. Lett. **86**, 5514 (2001).
[23]J. E. Gerbi, P. M. Voyles, M. M. J. Treacy, J. M. Gibson, J. R. Abelson, Appl. Phys. Lett. **82**, 3665 (2003).

Downloaded 11 May 2009 to 131.227.178.132. Redistribution subject to AIP license or copyright; see http://jap.aip.org/jap/copyright.jsp